Electromagnetic transitions between states satisfying free-boundary conditions

L. A. A. Nikolopoulos
Department of Telecommunication and Sciences, University of Peloponnisos, GR 22 100 Tripolis, Greece
(Received 30 September 2005; published 12 April 2006)

We address the problem of calculating electromagnetic transition matrix elements between states of a particle in spherically symmetrical potentials with no assumed boundary conditions at finite distance (free-boundary-condition method). For this, the Schrödinger equation is solved in a finite box of radius R and bound and continuum states, appropriately normalized, are numerically represented, through a variational finite-basis-set (B-spline) approach. The equivalence between the three transition operator forms (length, velocity, acceleration), within this approach, is discussed, and bound-continuum and continuum-continuum matrix elements are calculated in all three gauges. Results for the strong electromagnetic radiation of hydrogen are presented through the calculation of two-photon ionization cross sections and photoelectron angular distributions. It is demonstrated that the present approach is well suited for the calculation of multiphoton transitions when ionization in the continuum is allowed (above-threshold ionization). With the free-boundary-condition method complete control over the density of scattering states is feasible and, as the result of that, the degeneracy in the continuum between partial waves is preserved.

DOI: 10.1103/PhysRevA.73.043408 PACS number(s): 32.80.Rm

I. INTRODUCTION

A primary task in any theory of the interaction of electromagnetic (EM) radiation with atomic systems is an accurate and reliable description of the atomic or ionic structure, accomplished by solution of the corresponding Schrödinger equation (SE). Through the years a wide variety of methods have been developed and applied, each of them having its limitations which are context dependent. To refer to two of them, used most frequently for many years, we have the well-known Numerov method [1], consisting of direct integration of the radial SE on a grid, or the use of a finite basis set to expand the atomic states, with the most representative examples so far being the Gaussian or Slater functions. Both of these methods have been used mostly for a numerical representation of states belonging to the bound spectrum of the atomic or molecular Hamiltonians. On the other hand, scattering states (continuum spectrum) have been the subject of many theoretical or experimental studies over the past years, in both the context of atomic scattering and electromagnetic radiation theories. With the advent of high-power lasers, scattering states are commonly accessible. Indeed, use of the Numerov method (or variances of it) and methods based on Gaussian or Slater functions appear to be inappropriate since nonlinear phenomena involving continuum atomic states are necessary for their interpretation. At this point, we assume that it is neither necessary nor particularly useful to belabor here the significance of analyzing the scattering states in quantum physics. One of the most successful methods in atomic scattering theory has been proven to be the use of a finite basis set in conjunction with variational methods for representing the atomic states, belonging to either the bound or continuum spectrum [2–4]. By expanding the radial states on a set of known basis functions, with unknown coefficients to be determined, the differential equation is transformed into a matrix equation, solved by standard numerical techniques. The solutions corresponding to bound eigenstates, easily represented with high accuracy in a restricted part of the radial space, are normalized to unity. For solutions corresponding to scattering states, nonvanishing at infinity, arises the problem of the numerical representation together with the appropriate boundary conditions (BC's). While at the origin the BC's are set to zero, this is not the case at the other boundary of the radial space ($r \rightarrow \infty$).

One approach, hereafter called *fixed BC*, is to impose homogeneous artificial boundary conditions to a finite distance R of the form $\alpha P(R)+\beta P'(R)=0$, with $P(r)$ and $P'(r)$ being the radial eigenfunction and the derivative, respectively, resulting in an approximate finite representation of the true Hamiltonian inside this spherical box [5]. Those artificial boundary conditions provide the necessary link between the "interior" and "exterior" region set by the value R. For specific values of α and β the boundary constraint selects from the total spectrum of the allowed wave functions (bound and continuum) only those that this constraint fulfills. For bound states ($\epsilon<0$), the constraint forces a change in the function shape (prominent near the boundaries) together with an energy shift. For scattering states ($\epsilon \geqslant 0$), the continuous spectrum becomes a denumerable infinite subset of the physical one, since certain continuum discrete states are obtained. In other words the continuous spectrum has been discretized. In practice, however, a sufficiently dense discrete spectrum of positive solutions can be obtained which either does not pose any serious obstacle in the calculations or can be circumvented through certain methods (i.e., by repeating the calculations for slightly different box radii, interpolation within the energy spectrum, etc.) [2,3,6–9].

Turning now to the calculation of the electromagnetic transitions between the atomic states the most intriguing case is the transition between states that both belong to the continuum spectrum. The latter case has been studied under different contexts by many authors—to refer a few: within the R-matrix approach [10–13], multiphoton-ionization cross-section calculations [14,15], and time-dependent SE ap-

proaches [2,16,17]. The same problem has also been addressed by Nicolaides and co-workers when applying a state-specific approach to the solution of the time-dependent Schrödinger equation (TDSE) for a hydrogen atom under strong laser radiation [18,19]. The singularity occurring in the dipole matrix elements of continuum-continuum (cc) transitions as well as the contribution of the outer region ($R<r<\infty$) to the total matrix element, in a fixed BC approach, was also discussed by van Enk *et al.* [17]. van Enk *et al.* argue that, in the context of the TDSE, there is no need for the calculation of the "outer" contribution to the cc dipole matrix element provided that the duration of the pulse is such that the fastest electron, which is ionized, does not reach the boundaries during the interaction, meaning that the time-dependent wave function has negligible values out of the box.

In the context of lowest-order perturbation theory, for the calculation of the multiphoton transition amplitude, there is a need to perform intermediate summations over the bound and continuum spectra. These summations involve matrix elements between bound-continuum and cc states. It is the latter to which special attention should be shown, given the infinite extension of the continuum states. In fixed-BC approaches the system is strictly confined in a restricted space (spherical box or radius R). For instance, Tang and Chang [6] assume an infinite-height potential at the boundaries by simply choosing only the wave functions that relax at the box boundaries $[P(R)=0]$. This confinement in the box leads to an uncontrollable discretization of the continuum spectrum. This is crucial in a number of cases such as the following: (a) when a very fine resolution of the scattering spectrum is necessary since the density of the continuum states is basically determined by the size of the box (R)—a fine energy spectrum is obtained either by enlarging the box radius or by repeating the calculations for several slightly different radii—(b) when above-threshold ionization (ATI) takes place—namely, when photon absorption occurs in the continuum spectrum, thus leading to a pole at the multiphoton transition amplitude. The difficulty here arises from the fact that, for a given box radius, the discrete energies does not necessarily match the continuum energies at the poles [3]. Again, one overcomes this difficulty by varying the box size until an eigenenergy coincides with the required pole or by adding an imaginary part to the pole [20]. In addition, the presence of the pole gives an imaginary part to the transition amplitude which involves an isolated cc matrix element, whose calculation necessitates the contribution from the outer region of the box [3,21]. (c) Finally, when angular distributions for the ejected electron are calculated, in a partial-wave approach, there is the need for the summation of the multiphoton transition amplitudes to the various partial waves $l=0,1,2,\ldots$ at *the same final photoelectron energy*. This cannot be fulfilled in the fixed-BC methods since given the centrifugal potential $l(l+1)/r^2$ the discretization of the continua is different for different angular numbers. All the above difficulties can be avoided within the present method, mainly because we have the freedom to calculate the eigenstates at particular energies.

In this paper we present a method for the calculation of atomic states with no assumed boundary conditions (*free BC's*) on a finite polynomial basis (B-splines) as well as the calculation of transition matrix elements, between such free-boundary eigenstates. Similar work has already reported by Fischer and Idrees [22] which applies the Galerkin method for the calculation of continuum states for the hydrogen scattering problem as well as to photoionization of two-electron systems such as He and H^- [23]. Compared with these works we have extended the use of the method in the calculation of the cc transition matrix elements and applied to multiphoton processes in atomic systems. In a recent work, the present formulation of the cc dipole matrix elements has been applied successfully to multichannel quantum defect theory wave functions in calculating two-photon ATI cross sections of Xe and Ar [24]. The main properties of the B-spline polynomial basis and their use in atomic and molecular physics have reviewed in Ref. [3] where an extensive reference list of the related theoretical works can be found.

The organization of the paper is as follows: In Sec. II we discuss in detail the theoretical background for the calculation of bound and continuum eigenstates states of a particle in spherically symmetrical potentials. This includes the use of the B-spline basis set for the numerical description of the free-boundary states as well as the discussion for the appropriate normalization of the scattering states. In Sec. III the theory of electromagnetic transitions matrix elements, within the dipole approximation, is formulated for the three transition gauges: namely, the length, velocity, and acceleration gauges. In the last section, we calculate the two-photon ionization cross section, including ATI, from the hydrogen ground state and photoelectron angular distributions are presented for two kinetic energies of the ejected electron. These calculations involve matrix elements between continuum states, thus being a decisive test for the accuracy of the results. Atomic units are used throughout the text unless stated.

II. FREE-BOUNDARY-CONDITION METHOD

In the case of a particle subject to spherically symmetric potential the solution of the stationary Schrödinger equation can proceed as follows: Exploiting the spherical symmetry of the potential, the SE for the radial wave function is expressed as $[h_l(r)-\epsilon]P_{\epsilon l}(r)=0$ with [25]

$$h_l(r) = -\frac{1}{2}\frac{d^2}{dr^2} + \frac{l(l+1)}{2r^2} + V(r), \tag{1}$$

where $V(r)$ is a local potential obeying the asymptotic condition $\lim_{r\to\infty}(rV(r))=q_e$, with q_e being the charge of the atomic system "felt" by the particle at large distances. In addition, the above equation is supplemented with vanishing BC's at the origin for the radial wave functions: namely, $P_{\epsilon l}(0)=0$.

For the numerical solution of the atomic equations we introduce a parameter distance R $(0<R<\infty)$, thus effectively replacing infinity (∞) for a practical investigation of the problem. The most reasonable choice for the value of this boundary R is so large that its finite value introduces negligible error for all practical purposes with respect to the specific problem under consideration. The matrix representation

of the Hamiltonian results in a surface term evaluated at the point R. More specifically, the radial wave functions are expanded on the basis of B-spline polynomials as

$$P_{\epsilon l}(r) = \sum_{i=2}^{n_s} C_i^{(\epsilon l)} B_i(r), \tag{2}$$

where n_s is the number of polynomials $B_i(r)$. The B-spline polynomials $B_i(r)$, $i=1,2,\ldots,n_s$, of order k_s, are defined in an interval $[0,R]$ on a sequence of knot points $t[i] \leqslant t[i+1]$, $i=0,1,\ldots,n_s+k_s$, where $t[0]=t[1]=\ldots=t[k_s]=0$ and $t[n_s+1]=t[n_s+2]=\cdots=t[n_s+k_s]=R$ [26]. In the above expansion [Eq. (2)] the first B-spline polynomial (B_1) is excluded in order to ensure that $P_{\epsilon l}(0)=0$.

Substituting this expansion into the SE for the radial function $P_{\epsilon l}(r)$ and taking the variational condition, with respect to the coefficients $C_i^{(\epsilon l)}$, $\delta\langle B_j(r)|[h_l(r)-\epsilon]|\Sigma_i^{n_s} C_i^{(\epsilon l)} B_i(r)\rangle=0$, leads to the following matrix equation for the unknown coefficient vector $C_{\epsilon l}=(c_2^{(\epsilon l)}, c_3^{(\epsilon l)}, \ldots, c_{n_s}^{(\epsilon l)})$:

$$[\mathbf{h}^{(l)} + \mathbf{S} - \epsilon \mathbf{B}] \cdot \mathbf{C}_{\epsilon l} = 0, \tag{3}$$

with $\mathbf{h}^{(l)}$ being the symmetric part of the radial Hamiltonian [Eq. (1)], B the B-spline overlap matrix, and S the surface term, given by

$$h_{ij}^{(l)} = \frac{1}{2}\int_0^R dr \left[\frac{1}{2} B_i' B_j' + B_i \left(\frac{l(l+1)}{2r^2} + V(r) \right) B_j \right],$$

$$S_{ij} = -\frac{1}{2} B_i(R) B_j'(R),$$

$$B_{ij} = \int_0^R dr B_i(r) B_j(r).$$

Due to $B_i(R)=0$, $i \neq n_s$, and $B_{n_s}(R)=1$, the surface term is reduced only to terms with $i=n_s$. Finally from the properties of B-splines, we obtain the relation $B_{n_s}'(R)=-B_{n_s-1}'(R)=(k_s-1)/t_s$, with $t_s \equiv t[n_s+1]-t[n_s]=R-t[n_s]$. Then the only nonvanishing elements of the surface matrix S are the following two:

$$S_{n_s n_s} = -S_{n_s n_s-1} = \frac{1-k_s}{2t_s}. \tag{4}$$

This is a clearly unsymmetric matrix since $S_{n_s n_s-1} \neq S_{n_s-1 n_e}=0$. The degree of this nonsymmetricity can be controlled by varying certain parameters of the basis (n_s,k_s) and the knot sequence. This unsymmetric surface term and the overlap properties of B-spline polynomials ($\langle B_i|B_j\rangle=\delta_{ij}, |i-j|<k_s$) makes the matrix $\mathrm{h}^{(l)}+\mathrm{S}-\mathrm{B}$ on the left-hand side of Eq. (3) an $(n_s-1)\times(n_s-1)$ unsymmetric banded matrix of width equal to $2k_s+1$. For the solution of this matrix equation we follow two different approaches depending on the part of the spectrum we wish to calculate: namely, the bound and continuum ones.

A. Continuum spectrum

1. Calculation of the continuum eigenstates

By moving the surface term in the right-hand side (RHS) of Eq. (3) and making the transformation $\mathbf{C}_{\epsilon l} \rightarrow \mathrm{C}_{\epsilon l}/(C_{n_s-1} S)$, with $S=-S_{n_s n_s-1}$, we obtain the following system [23]:

$$[\mathbf{h}^{(l)} - \epsilon \mathbf{B}] \cdot \mathbf{C}_{\epsilon l} = \mathbf{C}_0, \tag{5}$$

where $\mathrm{C}_0 \equiv (0,0,\ldots,0,1)$. Therefore, we have rewritten the matrix equations keeping only the symmetric part of the Hamiltonian, thus making the system of linear equations nonhomogeneous. The non-Hermitian part of the Hamiltonian has moved to the RHS of the matrix equation, which in principle is *unknown*. Dividing both sides of equations by the *arbitrary* number $S \cdot C_{n_s-1}$ we fix the RHS as given by C_0. This way we have eliminated the problem of non-Hermiticity of the box Hamiltonian at the cost that we are only able to determine a solution vector of arbitrary normalization. Mathematically, the problem is an *initial-value problem*, leading to a family of solution vectors. By assuming a particular energy ϵ we solve the SE matrix equation as a linear system and obtain the solution, formally as $\mathbf{C}_{\epsilon l}=[\mathrm{h}^{(l)}-\epsilon \mathrm{B}]^{-1}\mathrm{C}_0$. Physically, by assuming no *boundary conditions* for the wave functions at the outer boundary, the atomic system is not confined in a box (as in fixed-BC methods) but extended to infinity, with the introduction of this "effective boundary" for numerical purposes. As already noted the obtained scattering states are known up to a multiplication factor. This factor will be determined through the conditions that the scattering states should satisfy at infinity.

2. Energy normalization and the scattering phase shifts

While for the bound states the normalization causes no problem, since they are orthonormal to unity, special care should be taken in the case of continuum states. By use of the asymptotic conditions satisfied by a particle in a Coulombing potential field we are able to renormalize the continuum states on the energy scale. For a radial SE in a central potential $V(r)$, the normalized solutions $P(r)$ asymptotically behave as [27]

$$\begin{aligned} P_{kl}(r) &= \sqrt{\frac{2}{\pi z(r)}} \sin[\phi(r) + \delta_l(k)] \\ &= F_{kl}(r)\cos\,\delta_l(k) + G_{kl}(r)\sin\,\delta_l(k), \end{aligned} \tag{6}$$

with $F_{kl}(r)$ and $G_{kl}(r)$ defined by inspection of Eq. (6). The "local" wave vector $z(r)$ satisfies the following differential equation:

$$z^2(r) = z_0(r) + z^{1/2} \frac{d}{dr}(z^{-1/2}), \tag{7}$$

with $z_0(r)=k^2/2-l(l+1)/2r^2-V(r)$. The phase $\phi(r)$ of the wave function is given as a solution of the first-order differential equation $\phi'(r)=z$, supplemented with the asymptotic condition $\phi(r\rightarrow\infty)\rightarrow kr-l\pi/2-q_e\ln(2kr)/k+\sigma_l(k)$, where $\sigma_l(k)=\arg\Gamma(l+1+iq_e/k)$ is the, analytically known, long-range Coulomb phase shift. We evaluate all the above equa-

tions in the region around $r \sim R$. The numerical calculation of $z(r)$ is performed through a second-order analytical iterative expansion [27].

Being able to calculate the function $z(r)$ and the phase $\phi(r)$, we assume that the physical solution $P_{kl}(r)$ differs from the calculated one $\bar{P}_{kl}(r)$ by a constant in space factor,

$$P_{kl}(r) = A_{kl}\bar{P}_{kl}(r). \tag{8}$$

Evaluating $F_{kl}(r)$ and $G_{kl}(r)$ from Eq. (6) and using the calculated values $\bar{P}_{kl}$ at the points $r_1, r_2 \sim R$, from Eq. (8) we obtain, for the short-range phase shift,

$$\tan \delta_l(k) = \frac{\bar{P}_{kl}(r_2)F_{kl}(r_1) - \bar{P}_{kl}(r_1)F_{kl}(r_2)}{\bar{P}_{kl}(r_1)G_{kl}(r_2) - \bar{P}_{kl}(r_2)G_{kl}(r_1)}. \tag{9}$$

Having calculated the short-range phase shift $\delta_l(k)$, we determine the renormalization factor as

$$A_{kl} \equiv \frac{1}{\bar{P}_{kl}(R)}\sqrt{\frac{2}{\pi z(R)}}\sin[\phi(R) + \delta_l(k)]. \tag{10}$$

At this point two important quantities have been determined: (a) the renormalization factor A_{kl} that transforms the calculated continuum wave functions into energy-normalized wave functions and (b) the short-range scattering phase shift $\delta_l(k)$.

B. Bound spectrum

The bound-state spectrum is obtained by setting $P(R)=0$. Physically, the above condition for the bound states is easily justified since their asymptotic behavior is as $P_{\epsilon l}(r \to \infty) \sim \exp(-\sqrt{2\epsilon}r)$ [25]. Thus, given the value of the box radius R, there are a number of bound states that are accurately represented by the requirement $P(R)=0$. This is achieved by excluding from the B-spline expansion [Eq. (2)] the last B-spline B_{n_s}, since $B_{n_s}(R)=1$ and $B_i(R)=0$, $n \neq n_s$, thus eliminating the surface term. Mathematically, this BC for the bound states defines a *two-point boundary-value* problem, whose solution give discrete eigenfunctions and eigenenergies. The matrix equation [Eq. (3)] is transformed into a banded generalized eigenvalue matrix problem of the following type:

$$\mathbf{h}^{(l)} \cdot \mathbf{C}_{\epsilon_n l} = \epsilon_{nl}\mathbf{B} \cdot \mathbf{C}_{\epsilon_n l}. \tag{11}$$

The solution vector for each partial wave $l=0,1,2,\ldots$ is obtained with standard matrix techniques, being very stable efficient, and accurate. The resulting radial functions satisfy the usual orthonormal relation $\langle P_{\epsilon_n l} | P_{\epsilon_{n'} l}\rangle = \delta_{\epsilon_n \epsilon_{n'}}$. The present approach is nothing else than the one we have called the fixed-BC method [6]. The main difference here is that we employ fixed BC's only for the bound spectrum. Note that a procedure, similar to the one followed for the continuum states, can also be applied to the bound spectrum by an inverse iteration algorithm.

III. ELECTROMAGNETIC TRANSITION OPERATORS

In this section we present the dipole transition operators as they transformed when we impose no BC's at the boundary R. The formulas $\hat{D}_L = r$, $\hat{D}_P = \nabla$, and $\hat{D}_A = \nabla V(r)$ represent the transition operators in the dipole (long-wavelength) approximation, for the length, velocity, and acceleration gauges, respectively. Assuming two eigenstates $\phi_a(r)$ and $\phi_b(r)$ of the Hamiltonian operator $[h = -\nabla^2/2 + V(r)]$, it can be the following relation can be shown [28]:

$$D_A = \epsilon_{ba}^2 D_L = \epsilon_{ba} D_P, \tag{12}$$

with $\epsilon_{ba} = \epsilon_b - \epsilon_a$, $h|i\rangle = \epsilon_i|i\rangle$, $i = a, b$, and $D_G = \langle a|\hat{D}_G|b\rangle$, $G = L, P, A$. The above equations are valid under the assumption that the Hamiltonian is Hermitian. In the present case where the Hamiltonian operator is non-Hermitian it is expected that the relationship between the gauges changes accordingly. From a practical point of view the problem of the calculation of the transition integrals can be expressed as follows: We only have a representation of the wave functions in a limited space $0 < r < R$. How can we calculate integrals that, in principle, extend to infinity? One solution is to neglect the region from R to ∞, assuming that the corresponding contribution is small compared with the "inner"-region contribution to the transition amplitude. That might be correct when one of the states belongs to the bound spectrum of the atomic system, since its wave function vanishes exponentially. However, in the case that both states belong to the continuum spectrum this is no longer necessarily true: since these states oscillate asymptotically the relevant integrals, for the length and velocity forms, extending up to infinity, can give a significant contribution to the total matrix element. The magnitude of this "outer" contribution, compared to the inner contribution, is dependent on the value R and the difference in energy between the scattering states. This problem becomes especially important when the energies of the continuum states approach each other: namely, when $\epsilon_a \to \epsilon_b$, since the relevant integral diverges. A procedure for calculating the outer-region contribution of the dipole transition integrals is presented below and based on related work by Peach [10] as well as by Seaton within the R-matrix framework [12,13]. Due to the spherical symmetry of the Hamiltonian, the eigenstates can be written as $\phi(r) = [P(r)/r]Y_{lm}(\theta, \phi)$, and assuming linearly polarized light along the z axis the transition matrix elements D_G are decomposed to a product of two quantities: namely $K(l_a, m_a; l_b, m_b)$ and $T_G(a,b)$, where $K(l_a, m_a; l_b, m_b) = \langle Y_{l_a m_a}|\cos\theta|Y_{l_b m_b}\rangle = \delta_{m_a m_b}\sqrt{(l_>^2 - m_a^2)/(4l_>^2 - 1)}$ with $l_> = \max(l_a, l_b)$ carrying common angular factors for all gauges and $T_G(a,b)$ being dependent on the radial wave functions alone [28,29]. The quantity $Y_{lm}(\theta, \phi)$ is the standard spherical harmonic function. The radial matrix element is given by

$$T_G(a,b) = \int_0^\infty dr P_a(r)\hat{T}_G(r)P_b(r), \tag{13}$$

with $\hat{T}_G$ the corresponding radial operator of each gauge. The radial operators for the velocity and acceleration gauges are

defined through the commutation relations $T_P=\langle a|(\hat{T}_L h_{l_b}-h_{l_a}\hat{T}_L)|b\rangle$ and $T_A=\langle a|(\hat{T}_P h_{l_b}-h_{l_a}\hat{T}_P)|b\rangle$, given that $\hat{T}_L=r$, resulting in [10,18]

$$\hat{T}_P=\left[\frac{\partial}{\partial r}+(l_b-l_a)\frac{l_>}{r}\right], \tag{14}$$

$$\hat{T}_A=\frac{dA}{dr}. \tag{15}$$

The radial integral [Eq. (13)] is separated into the inner T_G^I and outer T_G^O parts ($T_G(a,b)=T_G^I+T_G^O$), defined by the boundary R:

$$T_G^I=\int_0^R dr P_a(r)\hat{T}_G(r)P_b(r), \tag{16}$$

$$T_G^O=\int_R^\infty dr P_a(r)\hat{T}_G(r)P_b(r). \tag{17}$$

For convenience, we will discuss separately the calculation of the quantities T_G^I and T_G^O.

(*a*) *Inner-region contribution*: $0<r<R$. Due to the finite extension of the region of the integral, the calculation of the quantity T_G^I, with any standard integration technique is straightforward and presents no special difficulties even in the on-shell case $\epsilon_a=\epsilon_b$ for all three gauges.

(*b*) *Outer-region contribution*: $R<r<\infty$. It is the infinite extension of this integral that presents numerically difficulties which become especially severe when the eigenstates are degenerate ($\epsilon_a=\epsilon_b$) and both belong to the continuum spectrum. The most common choices for the calculation of EM transitions are the length and velocity gauge for a number of reasons so far. Unfortunately, these are the gauges that the outer radial integral might have a significant contribution to the total matrix element, when extending the calculation up to infinity. Indeed, in the most extreme case of equal energies ($\epsilon_a=\epsilon_b$) the corresponding integrals diverge. On the other hand, in the acceleration gauge, the convergence is obtained rather easily since the integral over the radial eigenstates contains a term that vanishes at least as $\sim 1/r^2$ (hydrogenic case). From this, it is concluded that the outer part of the dipole matrix element can be calculated in the acceleration gauge with high accuracy and contains no singularities. To obtain the total transition matrix element one should add the outer part (calculated in the acceleration gauge) to the inner part (calculated in the desired gauge) plus the surface contribution. Therefore it is necessary to determine the relation of the dipole matrix elements between the different gauges in the specific case of the non-Hermitian Hamiltonian arising from the use of free BC's. Such relations are obtained through the commutation relations between the different operators.

We again start from the commutation relations for the length, velocity, and acceleration gauges at the outer region by considering the integrals $T_P^O=\int_R^\infty dr P_a(r)(\hat{T}_L h_{l_b}-h_{l_a}\hat{T}_L)P_b(r)$ and $T_A^O=\int_R^\infty dr P_a(r)(\hat{T}_P h_{l_b}-h_{l_a}\hat{T}_P)P_b(r)$, resulting in

$$T_P^O=\epsilon_{ba}T_L^O-S_L, \tag{18}$$

$$T_A^O=\epsilon_{ba}T_P^O+S_P, \tag{19}$$

with S_L and S_P being the surface contributions at the boundaries,

$$S_L=\frac{1}{2}[rW_{ab}+P_aP_b]_{r=R}, \tag{20}$$

$$S_P=\frac{1}{2}\left\{P_a'P_b'+2\left[\epsilon_b-\frac{l_b(l_b+1)}{2r^2}-V\right]P_aP_b+(l_a-l_b)\frac{l_>}{r^2}(rW_{ab}-P_aP_b)\right\}_{r=R}, \tag{21}$$

with $W_{ab}(r)\equiv P_aP_b'-P_bP_a'$ being the Wronskian of $P_a(r)$ and $P_b(r)$. The contribution at infinity ($r\to\infty$) vanishes since, if one of the states is bound, then it goes to zero exponentially, or if both states are in the continuum, then they oscillate as a function of their energies and a strong cancellation occurs. The expression for S_P has simplified further by use of the radial SE [Eq. (1)]. From Eqs. (18) and (19) we obtain for the length and velocity forms the total radial integral as

$$T_L(a,b)=T_L^I+\frac{1}{\epsilon_{ab}^2}(\epsilon_{ba}S_L-S_P)+\frac{T_A^O}{\epsilon_{ab}^2}, \tag{22}$$

$$T_P(a,b)=T_P^I-\frac{1}{\epsilon_{ba}}S_P+\frac{T_A^O}{\epsilon_{ba}}. \tag{23}$$

Knowledge of the wave functions in the inner region $0<r<\infty$ allows an evaluation of the quantities T_L^I, T_P^I and the surface terms S_L, S_P. The outer-region integral T_A^O is a rapidly convergent integral since $V(r)$ vanishes as $1/r$ or faster. For instance, in the case of hydrogenic atomic system we have $V(r)=-Z/r$ and

$$T_A^O=\int_R^\infty P_a(r)\frac{Z}{r^2}P_b(r), \tag{24}$$

with Z being the atomic number. This integral is a smooth function of the energy difference ϵ_{ba} of the states $P_a(r)$ and $P_b(r)$ and for its evaluation we use the expansion [Eq. (6)] for $r>R$. Finally, it can easily be shown that the surface terms S_L and S_P vanish either when $R\to 0,\infty$, or when $P_a(R)$ and $P_b(R)$ are set to zero. The latter case is the approach followed from the method of fixed BC's.

IV. RESULTS AND DISCUSSION

In this section we apply the method to the hydrogen atom having a Coulomb-like potential ($\sim -1/r$), resulting in vanishing short-range scattering phase shifts for all partial waves $l=0,1,2,\ldots$ and all energies. The total [Eqs. (22) and (23)], inner [Eq. (16)], and surface [second term of Eqs. (22) and (23)] radial matrix elements are calculated in the length (Figs. 3–5) and velocity (Fig. 6) gauges. In the acceleration gauge the total [Eq. (13)] and the outer radial matrix elements [Eq. (24)] are also calculated (Fig. 7).

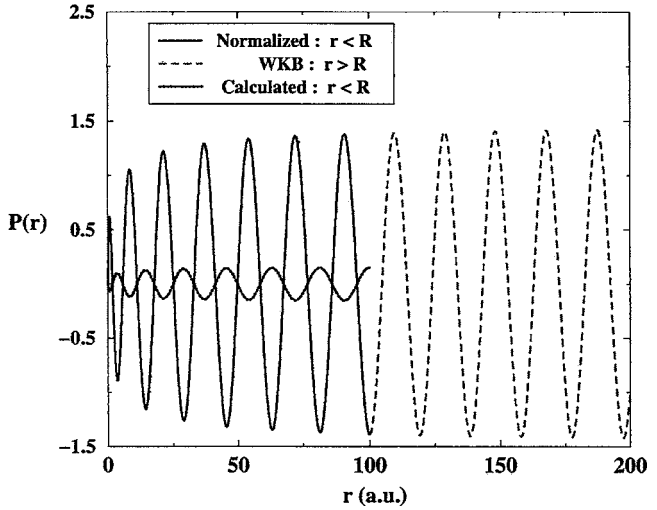

FIG. 1. Energy-normalized hydrogen continuum radial wave function for $\epsilon_k=0.045$ a.u. ($k=0.3$ a.u.) and $l=0$. Box radius is $R=100$ a.u. In the same plot the calculated radial wave function is plotted as well as the WKB radial wave function extended in distance up to 200 a.u.

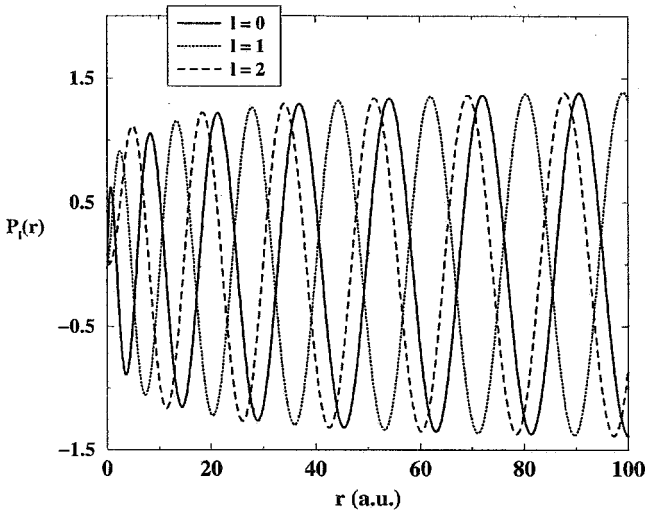

FIG. 2. Energy-normalized hydrogen radial wave functions at the same continuum energy $\epsilon_k=0.045$ a.u. for $R=100$ a.u. for the s,p,d partial waves.

A. Hydrogen radial wave functions

The hydrogen potential is given by $V(r)=-1/r$. We mostly present calculations involving scattering states since bound wave functions are easily calculated with high accuracy due to their finite extension. Initially in Fig. 1 we plot the hydrogen continuum partial radial wave function $P_{\epsilon s}(r)$ for $\epsilon=0.045$ a.u. (solid line). The box radius is chosen to be $R=100$ a.u. In this figure the calculated (unormalized) radial wave function is plotted together with the Wentzel-Krammers-Brillouin (WKB) radial wave function extended in distance up to 200 a.u. The energy normalized radial wave function is obtained applying the normalization procedure as presented in the related section. Use of the calculated radial wave function and WKB values at the box boundary $R=100$ a.u. results in the determination of the normalization factor [Eq. (10)]. The WKB wave function is the one as given by Eq. (6) with $\delta_l(k)=0$ and $q_e=-1$. One can notice that for $R=100$ a.u. the wave function has reached well its asymptotic limit, thus allowing an excellent matching of the WKB wave function and the calculated one. Use of either the numerical (energy-normalized) radial function or the WKB analytical function leads to practically identical results.

Next, in Fig. 2, we plot the energy-normalized hydrogen radial wave functions for the s, p, and d partial waves. The difference in phase of the wave functions at the boundary ($\sim l\pi/2$), between the partial waves $l=0,2$ and $l=1$, is consistent with the asymptotic form of the wave functions.

B. Hydrogen radial dipole matrix elements

In Fig. 3 we plot the inner-region contribution $0<r<R$ of the bound-free radial dipole matrix element T_L^I (length form) from the $P_{4s}(r)$ hydrogen state to the final $P_{\epsilon p}$ continuum for various box radii. As the box is enlarged the influence on the matrix element is gradually decreased (the amplitude of the oscillations as a function of the final energy) toward the value obtained when $R\to\infty$. It is also evident from the figure that not only the amplitude of the oscillations decreases as a function of the final energy, but in addition the "wavelength" of the oscillations increases. In the same calculation we have chosen $R=60$ a.u. to demonstrate the influence of the surface terms $(\epsilon_{ba}S_L-S_P)/\epsilon_{ba}^2$ on the total radial matrix element. This is shown in Fig. 4 where the total, inner-region, and surface dipole matrix elements are plotted. The outer-region contribution T_A^O/ϵ_{ba}^2 is about four orders of magnitude smaller than the above contributions and is not shown.

Similar behavior appears when both states are belonging to the continuum spectrum. Radial cc dipole matrix elements in the length (Fig. 5) and velocity (Fig. 6) gauges, from the $\epsilon_a=26.53$ eV (s-wave) initial state to the final $P_{\epsilon_b P}$ con-

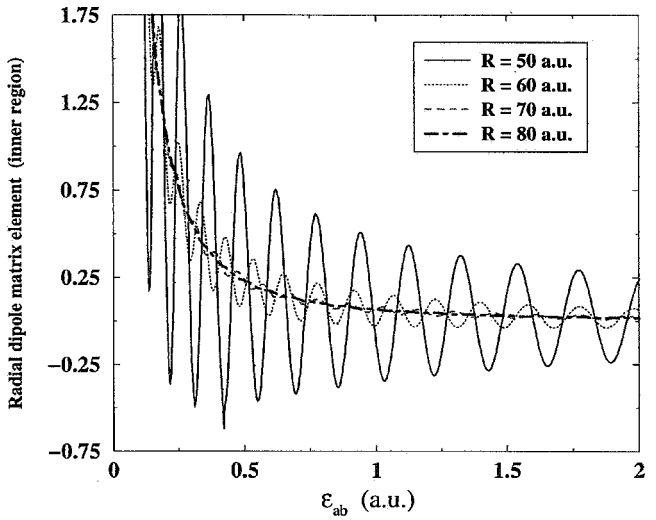

FIG. 3. Inner-region contribution of the radial dipole matrix element (length gauge) from the $4s$ hydrogen initial state ($\epsilon_a=-0.03125$ a.u.) to the final ($\epsilon_b p$) continuum states for various values of R.

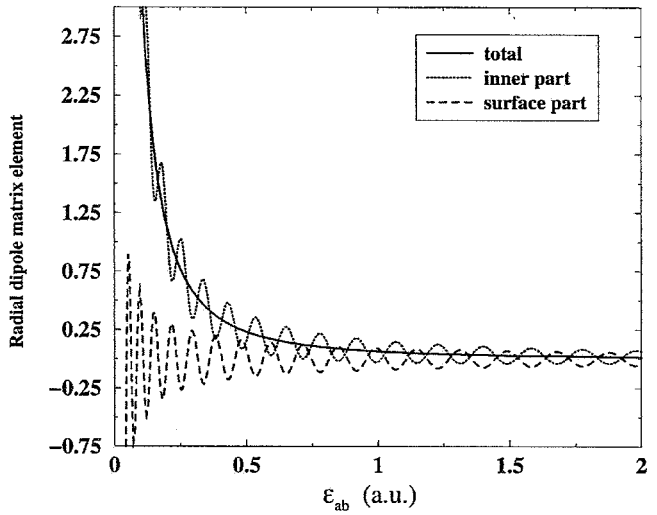

FIG. 4. Radial bound-continuum dipole matrix element (length gauge) from the $4s$ hydrogen initial state ($\epsilon_a = -0.03125$ a.u.) to the final ($\epsilon_b p$) continuum states for $R=60$ a.u. In the plot the total, inner-region, and surface part dipole matrix elements are shown.

tinuum, are shown. In the figures the total, inner-region and surface dipole matrix elements are plotted. The latter two contributions compensate for each other such that the value of the total matrix element results in a smooth decreasing function of the energy difference between the states. The outer-region contribution again is about four orders of magnitude smaller and is not shown. Note the divergence for transitions between degenerate states ($\epsilon_a = \epsilon_b$) in both forms. As in the bound-free case, the inner-region and surface terms oscillate with decreasing amplitude and increasing wavelength as a function of the energy difference ϵ_{ba}. In Fig. 7(a) we calculate the total radial matrix element in acceleration form. The singularity has disappeared, and convergence of the calculation is quickly reached due to the presence of the

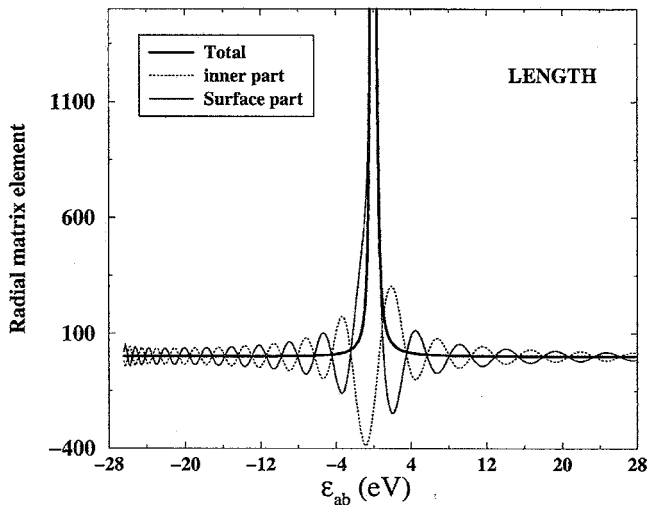

FIG. 5. Radial cc dipole matrix element (length gauge) from the $\epsilon_a s$ ($\epsilon_a = 26.53$ eV) hydrogen initial state to the final ($\epsilon_b p$) continuum states for $R=60$ a.u. In the plot the total, inner-region, and surface part dipole matrix elements are shown.

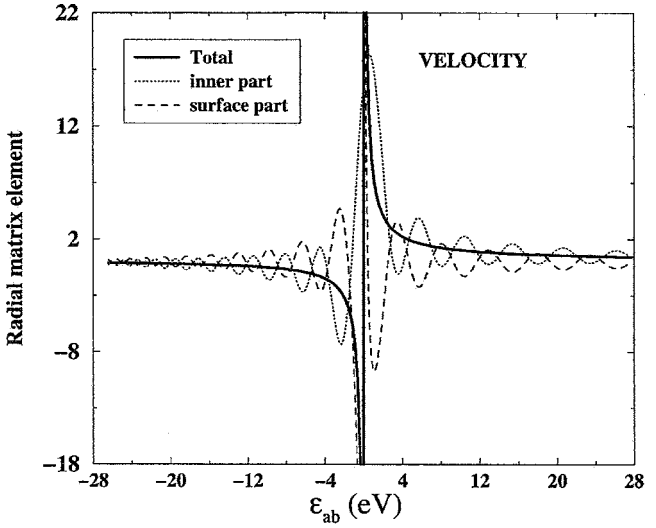

FIG. 6. Radial cc dipole matrix element (velocity gauge) from the $\epsilon_a s$ ($\epsilon_a = 26.53$ eV) hydrogen initial state to the final ($\epsilon_b p$) continuum states for $R=60$ a.u. In the plot the total, inner-region, and surface part dipole matrix elements are shown.

$1/r^2$ factor in the integral. In Fig. 7(b) the contribution of the outer region $R < r < \infty$ to the dipole matrix element [Eq. (24)] is also plotted, being three orders of magnitude smaller. The same quantities are also obtained with the use of the nonrelativistic Green function method as presented by Koval and Fritshze [30]. Agreement between the two approaches of the order of 10^{-6} has been achieved.

C. Two-photon photoelectron angular distribution and ionization cross section for hydrogen

An important test of the method is provided by the calculation of the two-photon ionization cross section. This quan-

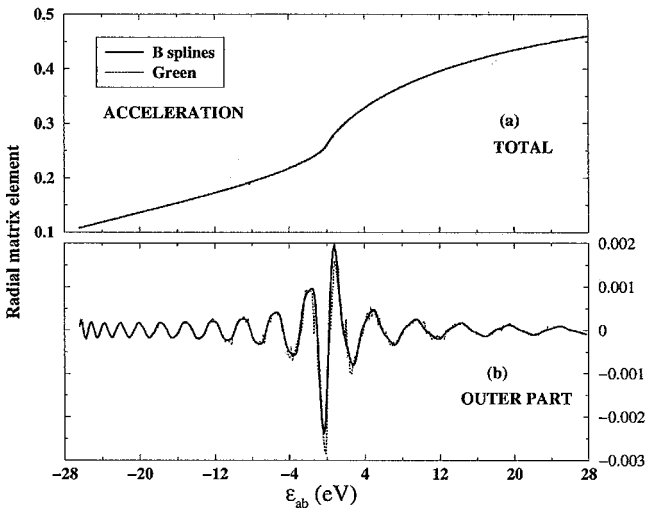

FIG. 7. (a) Total radial cc dipole matrix element in the acceleration gauge from the $\epsilon_a s$ ($\epsilon_a = 26.53$ eV) hydrogen initial state to the final ($\epsilon_b p$) continuum states for $R=60$ a.u. (b) The outer-region contribution (T_A^O), being about two orders of magnitude smaller, is shown. In the same plots, calculations with a Green function approach [30] are also shown. Except in the near-resonance region ($\epsilon_a \sim \epsilon_b$) the agreement is within the thickness of the lines.

tity involves matrix elements between scattering states (cc transitions), the accurate calculation of which is crucial for the final value.

Within the lowest-order perturbation theory [2,8], the photoelectron angular distribution (PAD) of a two-photon transition, by linearly polarized light along the z axis, from an initial state with $|i\rangle=|\epsilon_i,l_i,m_i\rangle$ to a final continuum state of energy $\epsilon_f=k_f^2/2$, satisfying incoming-wave boundary conditions [31], is given by

$$\frac{d\sigma_{if}^{(2)}}{d\Omega_{k_f}}(\epsilon_f,\theta_{k_f},\phi_{k_f})=C_2|M_G^{(2)}(\epsilon_f,\theta_{k_f},\phi_{k_f})|^2,$$

with G denoting the gauge used. Here $C_2=8\pi^3a^2\omega^2$, with a being the fine structure constant and ω the photon energy of the EM field. The angle θ_{k_f} denotes the angle of ejection of the photoelectron with respect to the polarization axis of the EM field. By expanding the atomic states on a basis of spherical waves [32], we obtain

$$M_G^{(2)}(\epsilon_f,\theta_{k_f},\phi_{k_f})=\sum_{l_f=0,2}M_G^{(2)}(\epsilon_f l_f)Y_{l_fm_f}^*(\theta_{k_f},\phi_{k_f}),$$

$$M_G^{(2)}(\epsilon_f l_f)=i^{l_f}e^{-i\Delta_{l_f}(k_f)}T_G^{(2)}(\epsilon_f l_f)K_{l_fm_f}^{(2)}.$$

The phase shift $\Delta_{l_f}(k_f)$ is the sum of the Coulomb and short-range phase shifts: namely, $\Delta_{l_f}(k_f)=\sigma_{l_f}(k_f)+\delta_{l_f}(k_f)$. The angular amplitudes are equal to $K_{l_fm_f}^{(2)}=K(l_i,m_i;l,m)\times K(l,m;l_f,m_f)$ with l,m and l_f,m_f being the angular quantum numbers of the partial-wave expansion of the intermediate and final wave functions, respectively. The quantities $T_G^{(2)}(\epsilon_f l_f)$ are the two-photon radial matrix elements, involving a summation over the whole spectrum of the allowed bound $(\epsilon_n lm)$ and continuum (ϵlm) intermediate states,

$$T_G^{(2)}(\epsilon_f l_f)=\sum_{\epsilon_n\leqslant 0}\frac{T_G(\epsilon_i l_i,\epsilon_n l)T_G(\epsilon_n l,\epsilon_f l_f)}{\epsilon_i+\omega-\epsilon_n}+\int_0^\infty d\epsilon\frac{T_G(\epsilon_i l_i,\epsilon l)T_G(\epsilon l,\epsilon_f l_f)}{\epsilon_i+\omega-\epsilon},\qquad(25)$$

where $T_G(\epsilon_i l_i,\epsilon_n l)$, $T_G(\epsilon_n l,\epsilon_f l_f)$, $T_G(\epsilon_i l_i,\epsilon l)$, and $T_G(\epsilon l,\epsilon_f l_f)$ are the single-photon dipole matrix elements defined in Eq. (13) and calculated by the use of Eqs. (22) and (23), depending on the gauge used. The kinetic energy of the ejected photoelectron is connected with the initial-state energy through the photon energy as $\epsilon_f=\epsilon_i+2\omega$.

In the case of an initial state having $l_i=0$ and $m_i=0$, as the hydrogen ground state, we have $K_{00}^{(2)}=(1/3)\delta_{m_f0}$ and $K_{20}^{(2)}=(2/\sqrt{45})\delta_{m_f0}$. By definition, integration over the wave vector angles (here only over the θ_{k_f}) of $d\sigma_{if}^{(2)}/d\Omega_{k_f}$ results to the two-photon ionization cross section

$$\sigma_{if}^{(2)}(\epsilon_f)=\sum_{l_f=0,2}\sigma_{if}^{(2)}(\epsilon_f l_f)=C_2\left[\frac{1}{9}|T_G^{(2)}(\epsilon_f s)|^2+\frac{4}{45}|T_G^{(2)}(\epsilon_f d)|^2\right],$$

where $\sigma_{if}^{(2)}(\epsilon_f l_f)$, defined by inspection of the above formula, is the two-photon partial ionization cross section to the l_f angular symmetry.

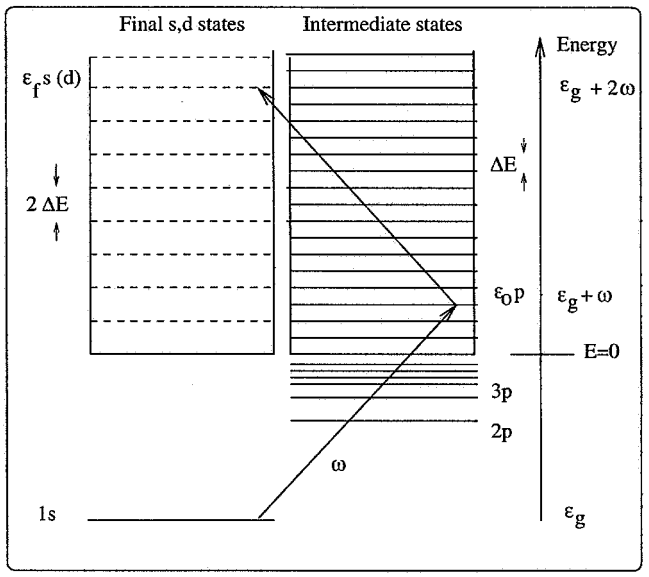

FIG. 8. Schematic figure for the numerical calculation of the two-photon ionization radial matrix elements in the ATI case.

1. Numerical integration of the two-photon transition amplitude $T_G^{(2)}$

The summation is over the bound intermediate states while the integral is performed over the continuum states of the p symmetry of the hydrogen atom. Within the free-BC method the continuum part of the two-photon transition amplitude can be evaluated with any numerical integration rule we want. This because the discretization of the continuum states can be chosen freely as has been described. In the calculation of the two-photon transition amplitudes an extra complication may arise when the photon energy of the EM field allows single-photon ionization (ATI case): namely, when $\epsilon_i+\omega=\epsilon$.

From the numerical point of view, a pole appears in the integrand with the behavior of a δ-function singularity. Within the present method, this anomaly is easily cured by choosing for the continuum intermediate states $(\epsilon_n>0)$ a discretization $\cdots<\epsilon_n<\epsilon_{n+1}<\cdots<\epsilon_{n_f}<\cdots$, with constant energy step equal to $\Delta E=\epsilon_{n+1}-\epsilon_n$ (see Fig. 8). Then, the discretization of the final states is chosen with a constant step $2\Delta E$. Thus, in the ATI case, for any of the final states $(\epsilon_{n_f}=\epsilon_i+2\omega)$ there is a corresponding intermediate state ϵ_{n_0} such that $\epsilon_{n_0}=\epsilon_i+\omega$. The pole is extracted from the integral [Eq. (25)] by use of the identity $\lim_{\eta\to 0}1/(x-i\eta)=P(1/x)+i\pi\delta(x)$, with P being the symbol of principal value. For instance, starting from the hydrogen ground state we have

$$T_G^{(2)}(\epsilon_f l_f)=\sum\!\!\!\!\!\!\int_{\epsilon_n\neq\epsilon_0}\frac{T(1s,\epsilon_n p)T(\epsilon_n p,\epsilon_{n_f}l_f)}{\epsilon_{1s}+\omega-\epsilon_n}+i\pi T(1s,\epsilon_{n0}p)T(\epsilon_{n0}p,\epsilon_{n_f}l_f),\qquad(26)$$

with $\sum\!\!\!\!\!\!\int$ denoting integration over the bound and continuum

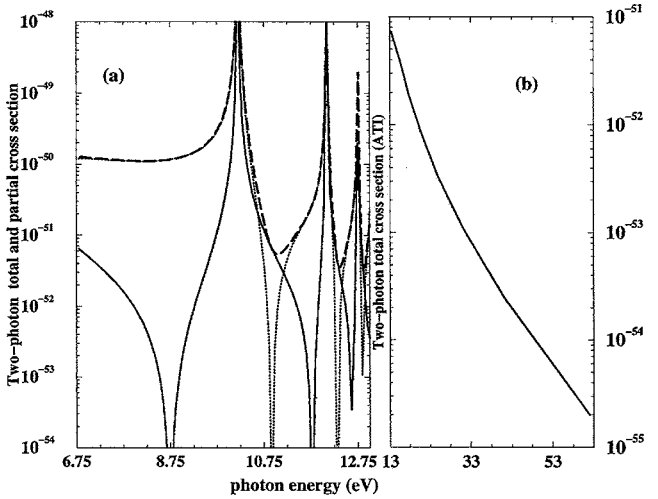

FIG. 9. (a) Two-photon partial ionization cross section from the hydrogen ground state for using the present free-BC method (*s*-wave, solid line; *d*-wave, dotted line). The total ionization cross section is also calculated, for comparison, with the Green function method as described in Ref. [30] (long-dashed line). The agreement of the present calculation of the total cross section with that of the Green function method is within the thickness of the line. (b) The two-photon total ionization cross section from the hydrogen ground state in the ATI regime.

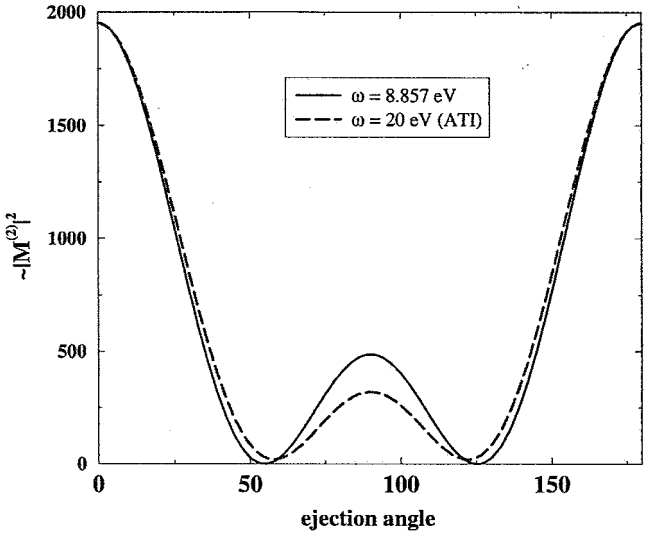

FIG. 10. Two-photon photoelectron angular distribution (arb. units) from the hydrogen ground state, as a function of the ejection angle (in deg) with respect to the polarization axis of the EM field, using the present free-BC method for two-photon energies.

spectrum of the p symmetry and $l_f=0,2$. Each of the continuum states is normalized by the use of Eq. (10) and each of the dipole matrix elements has calculated by the use of Eqs. (22) and (23) depending on the gauge used. In the present case we have chosen a box radius of 60 a.u. and constant energy step for a continuum discretization equal to $\Delta E=0.005$ a.u. The number of bound states ($\epsilon_n<0$) was 7 and the number of the intermediate continuum states ($\epsilon_n>0$) 1200.

From related equations an accurate and reliable calculation of the angular distributions in the two-photon transition involves both (a) the evaluation of partial-wave two-photon matrix elements and (b) the determination of the partial-wave phase shifts *at the same photoelectron energy*. Up to now such a calculation, within the fixed-BC method, was rather cumbersome, since the lack of degeneracy for different angular symmetries is inherent in the calculational procedure. Different partial waves, due to the centrifugal term, result in different discretizations of the corresponding radial Hamiltonian. Interpolation procedures were applied to overcome this inconvenience in the PAD calculation. Needless to say, increasing the order of the ionization process (since the number of final channels increases accordingly) the interpolation procedure becomes even more difficult.

Results for the two-photon ionization partial cross sections for $l_f=0$ (solid line) and $l_f=2$ (dotted line) from the hydrogen ground state, for the non-ATI case, are presented in Fig. 9(a). For comparison, calculations have also been performed with the Green function method [30]. We find agreement within the thickness of the lines; thus, we present only results for the total two-photon cross section [Fig. 9(a)] obtained with the Green function method (long-dashed line). In the ATI regime the total two-photon cross section has been calculated for a range of photon energies and plotted in Fig. 9(b).

Finally in Fig. 10 we have plotted the PAD for the kinetic energy of the ejected electron $\omega=8.857$ eV and $\omega=20$ eV. All basic features are present in this plot. For ($\omega\sim 8.857$ eV) where the $l_f=2$ wave dominates, the electrons are ejected not only along the polarization axis ($\theta_{k_f}=0°,180°$) but also in the perpendicular direction ($\theta_{k_f}=90°$), with smaller probability. For photon energy $\omega=20$ eV, which corresponds to an ATI process, again the $l_f=2$ partial wave dominates and the behavior of the angular distribution has similar behavior. The ejection to angles 60° and 120° is close to zero but not completely vanishing due to the presence of the s component of the wave function.

V. CONCLUSIONS

In conclusion, we have given the basic theory as well as the corresponding formulas for calculating bound and scattering states of systems subject to spherically symmetric potentials with free BC's. For this we have employed a variational finite basis (B-spline) method and transformed the radial SE to a system of linear equations, allowing for efficient and accurate computation, with standard techniques. Use of B-splines results in matrices of banded structure of width of the order of the B-spline basis. In addition a method for the calculation of bound-continuum and continuum-continuum transition matrix elements in length, velocity, and acceleration gauges is formulated. The outer-region contribution of the matrix elements is calculated, invoking the acceleration form together with the surface term originating from the finite representation of the operators. The main advantages of the present method are the following: (a) it allows complete control of the density of states in any energy range

of the scattering spectrum and, due to this, (b) preserves the degenerate character of the scattering spectrum for various partial waves. The latter two achievements were the main drawbacks of methods based on introducing artificial BC's as has been explained in the text. Furthermore, the present method allows a generalization of the B-spline method to more complicated systems involving multichannel states [33]. Such a multichannel method has been employed successfully in a typical three-body atomic system: namely, the helium atom [2,34]. In those works the single-electron orbitals were produced by a fixed-BC method, thus leading to complications related with to the degeneracy between the partial waves for each electron, a fact that we hope to solve with employment of the present approach.

[1] C. F. Fischer, *The Hartree-Fock Method for Atoms* (John Wiley & Sons, New York, 1977).
[2] P. Lambropoulos, P. Maragakis, and J. Zhang, Phys. Rep. **305**, 203 (1998).
[3] H. Bachau, E. Cormier, P. Decleva, J. E. Hansen, and F. Martin, Rep. Prog. Phys. **64**, 1601 (2001).
[4] F. Martin, J. Phys. B **32**, R197 (1999).
[5] B. W. Shore, J. Phys. B **7**, 2502 (1974).
[6] T. Chang and X. Tang, Phys. Rev. A **44**, 232 (1991).
[7] T. Chang, *Many-Body Theory of Atomic Structure* (World Scientific, Singapore, 1993), pp. 213–247.
[8] L. A. A. Nikolopoulos and P. Lambropoulos, Phys. Rev. A **56**, 3106 (1997).
[9] L. A. A. Nikolopoulos, Comput. Phys. Commun. **150**, 140 (2003).
[10] G. Peach, Mon. Not. R. Astron. Soc. **361**, 130 (1965).
[11] K. L. Bell, P. Burke, and A. Kingston, J. Phys. B **10**, 3117 (1977).
[12] M. J. Seaton, J. Phys. B **14**, 3827 (1981).
[13] M. J. Seaton, J. Phys. B **19**, 2601 (1986).
[14] M. Aymar and M. Crance, J. Phys. B **13**, L287 (1980).
[15] V. Veniard and B. Piraux, Phys. Rev. A **41**, 4019 (1990).
[16] X. Tang, T. Chang, P. Lambropoulos, S. Fournier, and L. DiMauro, Phys. Rev. A **41**, 5265 (1990).
[17] S. J. van Enk, J. Zhang, and P. Lambropoulos, J. Phys. B **30**, L17 (1997).
[18] T. Mercouris, Y. Komninos, S. Dionissopoulou, and C. Nicolaides, Phys. Rev. A **50**, 4109 (1994).
[19] T. Mercouris, Y. Komninos, S. Dionissopoulou, and C. Nicolaides, J. Phys. B **29**, L13 (1996).
[20] E. Cormier and P. Lambropoulos, J. Phys. B **28**, 5043 (1995).
[21] E. Cormier, H. Bachau, and J. Zhang, J. Phys. B **26**, 4449 (1993).
[22] C. F. Fischer and M. Idrees, Comput. Phys. **23**, 53 (1989).
[23] T. Brage, C. F. Fischer, and G. Miecznick, J. Phys. B **25**, 5289 (1992).
[24] T. Nakajima and S. Watanabe, Phys. Rev. A **70**, 043412 (2004).
[25] A. Messiah, *Quantum Mechanics* (Dover, Mineola, NY, 1999).
[26] C. de Boor, *A Practical Guide to Splines* (Springer-Verlag, New York, 1978).
[27] A. Burgess, Proc. Phys. Soc. London **81**, 442 (1963).
[28] I. Sobel'man, *Introduction to the Theory of Atomic Spectra* (Pergamon Press, Oxford, 1972).
[29] R. Cowan, *The Theory of Atomic Structure* (University of California Press, Berkeley, 1981).
[30] P. Koval and S. Fritzsche, Comput. Phys. Commun. **152**, 191 (2003).
[31] A. F. Starace, *Corpuscles and Radiation in Matter I*, Vol. 31 of *Handbuch der Physik* (Springer-Verlag, Berlin, 1982), pp. 1–121.
[32] L. A. A. Nikolopoulos, Phys. Rev. A **71**, 033409 (2004).
[33] H. W. van der Hart, J. Phys. B **30**, 453 (1997).
[34] L. A. A. Nikolopoulos and P. Lambropoulos, J. Phys. B **34**, 545 (2001).